A multiple-fibre diffusion phantom for the validation of HARDI methods

Ezequiel Farrher[1], Farida Grinberg[1], A. Avdo Celik[1], Kaveh Vahedipour[1], and N. Jon Shah[1,2]

[1]*Institute of Neuroscience and Medicine 4 - Medical Imaging Physics, Forschungszentrum Jülich, Jülich, Germany,* [2]*Department of Neurology, Faculty of Medicine, JARA, RWTH Aachen University, Aachen, Germany*

Target audience. We present a multiple-fibre anisotropic phantom for diffusion MRI applications. It is of great importance for scientists investigating high angular resolution diffusion imaging (HARDI) methods and fibre tracking algorithms, as well as molecular diffusion in biological tissue.

Purpose. Anisotropic fibre phantoms have become an indispensable tool in diffusion MRI, particularly in the validation of HARDI methods[1]. In this work we present a new design for anisotropic multiple-fibre phantoms. The most valuable feature of the new design is the integration of several geometrical configurations and fibre populations in a single device. An application of the phantom in the analysis of HARDI data using the so-called constrained spherical deconvolution[2] (CSD) approach was carried out, and the effect of self-induced susceptibility gradients was investigated.

Methods. The phantom was built using hydrophobic polyethylene fibres (Dyneema® DTX70) of 8 μm radius, wound around a Plexiglas® support (Fig.1)[1]. It includes four regions with different interwoven fibre configurations: one region contains a single fibre orientation with uniform fibre density (FD) (blue ROI); two regions contain interwoven fibres with different orientations at a distribution of angles in the range $50° < \varphi < 90°$ and with variable FD (black ROIs); a fourth region with triple-crossing fibres (red ROI). Dashed arrows in Fig.1 denote the fibre direction in each ROI. The whole setup was immersed in a cylindrical container filled with distilled water. Measurements were performed with a 3T Siemens Magnetom Trio scanner (Siemens, Erlangen, Germany). A spin-echo, multi-contrast sequence was used to evaluate FD[1]. A twice-refocused spin-echo, diffusion-weighted EPI sequence was performed for 256 gradient directions and *b*-values 0, 1000, 2000 s/mm^2. Evaluation of the fibre orientation distribution[2] (FOD) in the different areas was done with ExploreDTI[3]. Three maximum spherical-harmonic orders were considered in the analysis: l_{max} = 8, 10 and 12.

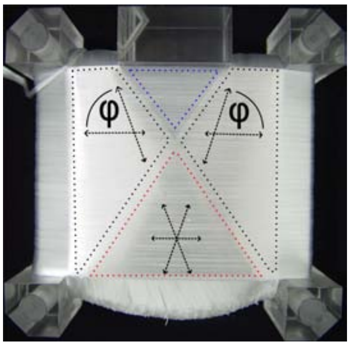

Figure 1. Photograph of the phantom showing the configurations: single-fibre (blue dots), double-fibre (black dots) and triple-fibre (red dots). Arrows in each area denote the fibre direction.

Results and discussions. Fig. 2a shows the map of FD from a selected slice. One can see that while the single- and triple-fibre regions have approximately uniform FD, the double-fibre has a variable FD. Results from the CSD analysis are shown in Fig. 2 for b = 1000 s/mm^2 (b,c,d) and b = 2000 s/mm^2 (e,f,g) and for l_{max} = 8 (b,e), 10 (c,f) and 12 (d,g). The results are overlaid on the FD maps. The colour of the cylinders representing the normalized maxima of the FODs refers to the number of resolved fibre directions in a given voxel: red, one fibre; green, two fibres; cyan, three fibres. Fig. 2a shows the orientation of the static magnetic field, $\boldsymbol{B}_0$, with respect to the fibres.

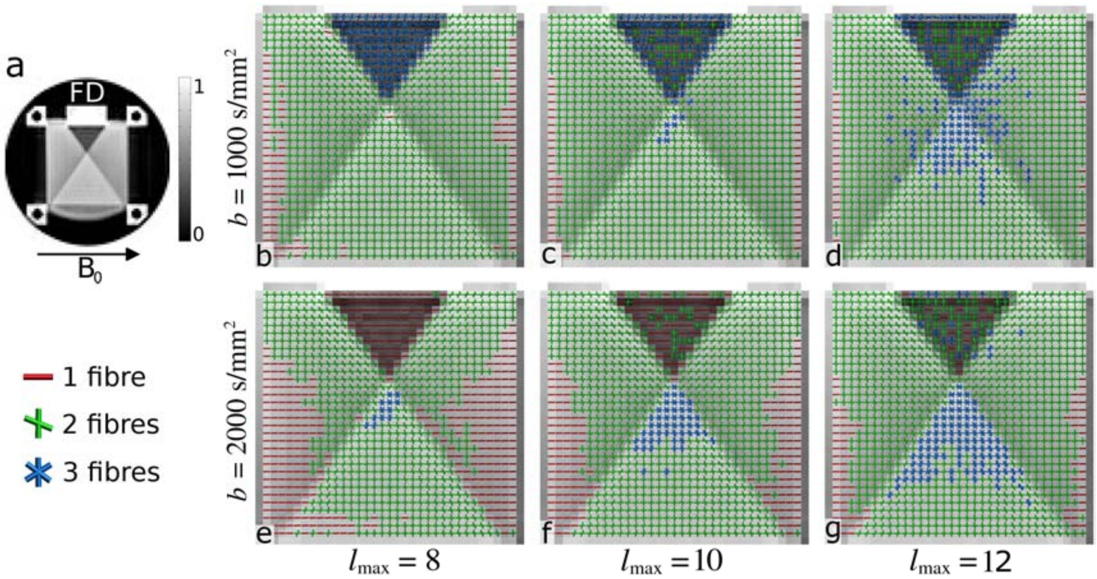

Figure 2. Map of FD (a). Cylinders representing the maxima of the normalized FODs obtained with the CSD method using *b*-values 1000 s/mm^2 (b,c,d) and 2000 s/mm^2 (e,f,g). The maximum spherical harmonics are: l_{max} = 8 (b,e), 10 (c,f) and 12 (d,g).

Single fibre: in Fig. 2, one can observe that for b = 1000 s/mm^2 (b,c,d) the resolved fibre directions show several artefacts due to the low FD. However, for b = 2000 s/mm^2 (e,f,g), the artefacts are reduced due to the fact that at higher *b*-value the signal from the bulk water is already attenuated.

Double fibre: here, one of the fibre populations is parallel to $\boldsymbol{B}_0$ and the other has an angle θ with $\boldsymbol{B}_0$ in the range $50° < \theta < 90°$. One can see that when $\theta \rightarrow 90°$, only the fibres parallel to the field are resolved (red cylinders), due to the fact that self-induced susceptibility gradients become stronger when the fibres are perpendicular to the magnetic field. In that case, only increasing the values of FD allows the resolution of the actual two fibres. This effect is stronger for b = 2000 s/mm^2 than for b = 1000 s/mm^2. On the other hand, increasing l_{max} significantly improves the resolution of fibre directions.

Triple fibre: it is shown that for b = 1000 s/mm^2 (b,c,d) only two fibre directions are resolved. However, as has been already discussed[2], increasing the *b*-value, in this case to 2000 s/mm^2 (e,f,g), allows a better resolution of multiple fibres (cyan cylinders) in some voxels, although it still fails in some others. Increasing l_{max} clearly improves the resolution of multiple fibres as well (Figs. 2e, f and g), although at low *b*-values and large l_{max}, CSD is susceptible to artefacts, as shown in Fig. 2d.

Conclusions. The new design combines several useful features in a single phantom; a single-fibre region with constant FD, two double-fibre areas with a distribution of crossing angle and variable FD, and a triple-fibre region with uniform FD. It was shown that CSD performs better at high *b*-value in the resolution of multiple fibres (especially 3 fibres). However, special attention needs to be paid to experiments performed in the presence of strong susceptibility background gradients (fibres nearly perpendicular to the magnetic field). In that case high diffusion weightings can lead to a miss estimation of the number of fibres. We are currently investigating the effect of such background gradients.

Acknowledgements. EF thanks Dr. A. Leemans for his help with the ExploreDTI toolkit and Dr. I.I. Maximov for useful discussions.

References. [1] E. Farrher, J. Kaffanke, A.A. Celik, T. Stöcker, F. Grinberg, N.J. Shah, *Magn. Reson. Imaging* 30, (2012) 518-526; [2] J.-D. Tournier, F. Calamante, A. Connelly, *Neuroimage* 35, (2007) 1459-1472. [3] A. Leemans, B. Jeurissen, J. Sijbers, D.K. Jones, *Proc. Intl. Soc. Magn. Reson. Med*. 17, (2007) 3537.